Distribution Agreement

In presenting this thesis as a partial fulfillment of the requirements for a degree from Emory University, I hereby grant to Emory University and its agents the non-exclusive license to archive, make accessible, and display my thesis in whole or in part in all forms of media, now or hereafter now, including display on the World Wide Web. I understand that I may select some access restrictions as part of the online submission of this thesis. I retain all ownership rights to the copyright of the thesis. I also retain the right to use in future works (such as articles or books) all or part of this thesis.

Austin Yu April 14, 2020

Bioprinting Extracellular Matrix Scaffolds as a Potential Treatment for Volumetric Muscle Loss

by

Austin Yu

Dr. Nick Willett
Adviser

Department of Biology

Dr. Nick Willett
Adviser

Dr. Hyojung Choo
Committee Member

Dr. Iain Shepherd
Committee Member

2020

Bioprinting Extracellular Matrix Scaffolds as a Potential Treatment for Volumetric Muscle Loss

by

Austin Yu

Dr. Nick Willett
Adviser

An abstract of
a thesis submitted to the Faculty of Emory College of Arts and Sciences
of Emory University in partial fulfillment
of the requirements of the degree of
Bachelor of Science with Honors

Department of Biology

2020

Abstract
Bioprinting Extracellular Matrix Scaffolds as a Potential Treatment for Volumetric Muscle Loss
By Austin Yu

Volumetric Muscle Loss is characterized by a loss of at least 20% muscle mass and muscle functionality. Because current treatments do not replace muscle function, the need for tissue regeneration therapies persists. Decellularized extracellular matrix (dECM) derived from host tissue-type offers a potential solution to providing a tissue environment suitable for myoblast differentiation but lacks the proper stiffness and physical organization for functional muscle growth. Gelatin Methacrylate (GelMA) along with 3D-bioprinting has been used to create a stiffer, printable biomaterial that facilitates nutrient transport and cell alignment. We hypothesized that GelMA biomaterial would contain similar structural protein content and stiffness to native muscle tissue and serve as a biomaterial scaffold for myoblast proliferation. Our overall objective was to develop a new dECM-GelMA hydrogel biomaterial that contained key structural cures for C2C12 myoblast proliferation. DNA quantification confirmed the removal of nucleic material following decellularization at <0.005 ng/mg, and mechanical testing found the stiffness of dECM-GelMA at 5.4 kPa to be similar to muscle tissue at 4.9 kPa. Immunohistochemical staining for collagen I and laminin in dECM and dECM-GelMA detected collagen I in dECM-GelMA. Laminin was detected in dECM but not in the hydrogel, prompting the need for future protein quantification. Cell proliferation assays measuring cell density in dECM and dECM-GelMA coated wells demonstrated similar proliferation to a collagen I positive control after 24 hours. A proliferation assay in dECM-GelMA printed patches also displayed increased proliferation after 72 hours. These promising data demonstrate the potential efficacy of dECM-GelMA as a scaffold for muscle progenitor cells and could be used in future work as a treatment for VML injury.

Bioprinting Extracellular Matrix Scaffolds as a Potential Treatment for Volumetric Muscle Loss

By

Austin Yu

Dr. Nick Willett
Adviser

A thesis submitted to the Faculty of Emory College of Arts and Sciences
of Emory University in partial fulfillment
of the requirements of the degree of
Bachelor of Science with Honors

Department of Biology

2020

Acknowledgements

I would like to thank Dr. Nick Willett, for the opportunity to work in his lab and invaluable expertise and guidance as my mentor. In addition, I would like to thank Willett Regenerative Labs, in particular Shannon Anderson, Fabrice Bernard, Emily Devereaux, Travis Fulton, Dr. Jarred Kaiser, and Dr. Anna McDermott who each dedicated their own unique expertise and time in making this project possible. Furthermore, I would like to thank the Dr. Liqun Ning from the Serpooshan Lab and Donald Bejleri from the Davis Lab, for the use of their facilities and guidance. I would also like to thank my other committee members. Dr. Hyojung Choo and Dr. Iain Shepherd for their continued support and incredibly valuable feedback. Finally, I would like to thank my friends and family for their continual support, humor, and care.

Table of Contents

List of Figures

Introduction

Volumetric Muscle Loss

Volumetric Muscle Loss (VML) is characterized by a large skeletal muscle trauma resulting in the deficit of at least 20% muscle mass (Grasman, Zayas, Page, & Pins, 2015).(Grasman, Zayas, Page, & Pins, 2015) VML muscle injuries can stem from a variety of traumas including, surgical procedures and extremity injuries on the battlefield. VML can significantly hinder muscle functionality, drastically impacting patient quality of life. Because of the sheer scale of the injury, the innate skeletal muscle repair mechanism is unable to effectively regenerate the lost muscle (Y. J. Choi et al., 2016). Currently, the treatment for VML is the use of autologous muscle graft, whereby muscle tissue is transplanted from another location on the patient's body to cover the damaged area (Kim et al., 2018). However, the donor site does not always provide sufficient muscle tissue to cover the entirety of the injury and in donor site morbidity.(Lee et al., 2020) In addition, the inevitable formation of fibrotic scar tissue further decreases muscle strength and function, requiring the need for alternative treatment methods that can improve muscle structure and function compared to current muscle graft treatments (Grasman et al., 2015). Currently, there are no treatments to completely restore muscle functionality, presenting the necessity to develop treatment strategies(Grasman et al., 2015).

Muscle Tissue Regeneration

In muscle reconstruction, muscle stem cells (MuSC), also known as satellite cells, play a vital role in the regenerative process of muscle tissue. Due to the regenerative capacity of MuSCs, they are a sought-after therapeutic cell type to treat muscular injuries (Wang, Dumont, & Rudnicki, 2014). Upon activation, which can occur in response to injury, MuSCs can differentiate into myogenic progenitor cells, or myoblasts, which further give rise to myotubes,

eventually leading to muscle fibers. Despite the promising use of MuSCs in treating muscular dystrophies, significant challenges still remain in maintaining a long-term suitable environment for MuSC viability (Wang et al., 2014). Previous work suggests that maintaining a microenvironment similar to the muscle stem cell niche, including proteins found within the extracellular matrix (ECM), may lead to successful MuSC survival and renewal (Bentzinger, Wang, Dumont, & Rudnicki, 2013). As a model in this study, we used C2C12 myoblasts, a mouse myogenic progenitor cell line, as a substitute for primary MuSCs.

dECM as a Biomaterial Treatment Option for VML

Decellularized extracellular matrix (dECM) consists of the structural elements isolated from the cellular components of a tissue extracellular matrix (ECM) using chemical tissue digestion (Lee et al., 2020). The main composition of ECM include fibrous-forming proteins, such as collagens, elastin, fibronectin (FN), laminins, glycoproteins, proteoglycans (PGs), and glycosaminoglycans (GAGs) (Sackett et al., 2018). However, the type and amount of these macromolecules will vary between different matrix types. Laminin critically contributes to cell attachment and differentiation, cell shape and movement, maintenance of tissue phenotype, and promotion of tissue survival. Fibronectin, which binds to integrin receptor proteins and collagen, contains an arginine, glycine, and aspartate tripeptide motif shown to mediate cell attachment, vital for necessary for cell growth, differentiation, and proliferation (Theocharis, Skandalis, Gialeli, & Karamanos, 2016). PGs, characterized by GAG carbohydrate chains linked to protein backbones has not only been demonstrated to bind other protein components such as laminin and collagen, but have also been demonstrated to upregulate during C2C12 myogenesis (Melo, Carey, & Brandan, 1996).

dECM can be used to form a hydrogel: a natural or synthetic polymer material with >30% water by weight (Sackett et al., 2018). Because dECM is also derived from the native tissue, it most closely resembles the structural organization already present within the host tissue, which is important in order for integration of dECM back into the host (Vorotnikova et al., 2010). In the case of dECM hydrogels, collagen polymers are responsible for hydrogel self assembly process at 37°C following pH neutralization. These dECM hydrogels can be injected direct into irregularly shaped defects or fabricated into specific structures through 3D-printing (Spang & Christman, 2018). Furthermore, dECM in a porcine derived matrix is reported to modulate macrophage responses to muscle injury, switching from an inflammatory response, to a tissue remodeling response in a VML tibialis anterior defect model (Aurora, Roe, Corona, & Walters, 2015) (Brown, Valentin, Stewart-akers, Mccabe, & Badylak, 2009).

However, despite its numerous benefits, a significant challenge with utilizing dECM scaffolds alone is creating functional muscle tissue. On its own, dECM scaffolds contain a randomly aligned, porous structure which largely results in creating misaligned muscle fibers and fibrotic scar tissue (Aurora et al., 2015). Without aligned muscle fiber regeneration, dECM is unable to restore overall muscle function. Therefore, a need persists to investigate further strategies for cell guidance.

3D Bioprinting using dECM

Recently, 3D bioprinting have had significant technological advancements allowing for many biomaterials to be used to create complex, intricate shapes to better replicate tissue structure. Bioprinting operates through the use of “bioinks” which are biodegradable tissue-derived or synthetic materials designed to maintain cell adhesion, differentiation, and proliferation, while maintaining a structural integrity suitable for printing(Pati et al., 2014).

While there are many different bioprinting techniques, conventional extruder-based bioprinters utilizes air pressure to carefully dispense the bioink from a nozzle into a 3D-modeled shape in a layer-wise fashion. To support the weight of the construct, structural supports such as polycaprolactone (PCL) can be used to maintain the shape and integrity of the construct (Kim et al., 2018). Since muscle function requires the organized contraction of muscle fibers, bioprinting aligned fibers improves muscle functionality in printed constructs. The high resolution of 3D bioprinted materials also allows channels to be created for nutrient infiltration, necessary for long-term stem cell viability (Y. Choi et al., 2019) (Bejleri et al., 2018). These resulting scaffolds offer vital support and direction for stem cell differentiation, creating aligned and functional muscle fibers (Y. Choi et al., 2019).

Despite the benefits of dECM in supporting MuSC differentiation and proliferation, there are limitations to its applications in bioprinting. One of the challenges of to print dECM hydrogels is dECM lacks sufficient structural integrity and requires a sacrificial non-biodegradable structural support, increasing handling difficulty and isolation from the support (Bejleri et al., 2018). In order to print dECM without support structures, researchers have tried to increase the density of dECM, which has proven to still be unstable when handling the material, risking rupture of the construct. Biodegradable structural support such as PCL has also been tested. However, PCL has been demonstrated to have mechanical mismatch with dECM, also resulting in a longer than optimal degradation time than dECM (Bejleri et al., 2018).

Gelatin Methacrylate as a Biocompatible Support

The structural limitations of dECM requires a biocompatible material that allows for similar cell differentiation and proliferation while increasing the stiffness suitable for printability and handling. Gelatin Methacrylate (GelMA) is a collagen-based biomaterial that contains

methacrylate and methacrylamide groups attached that allow for radical polymerization into a hydrogel (Yue et al., 2016). Due to its similar collagen components to dECM, GelMA allows for cell proliferation and is highly biocompatible with similar degradation times (Bejleri et al., 2018). In the gelation process, GelMA can also incorporate a visible light polymerization system using the photosensitizer eosin Y, initiator triethanolamine (TEA), and catalyst 1-vinyl-2 pyrrolidinone (NVP) (Bahney et al., n.d.) (Noshadi et al., 2017). Previous studies have determined that optimal C2C12 differentiation occurred at a similar stiffness to muscle tissue (Engler et al., 2004). By adjusting the concentration of GelMA, the hydrogel is able to match muscle tissue stiffness allowing for successful C2C12 myogenic differentiation (Ostrovidov et al., 2014). Finally, the stiffness of GelMA is essential for bioprinting, providing the structural support for dECM when creating three-dimensional constructs. However, it is important to note that GelMA, while a promising material for cell proliferation and differentiation, does not include the same bioactive and structural molecules as dECM. The muscle-tissue derived dECM remains necessary to match the microenvironment of muscle tissue for successful muscle tissue regeneration. For this reason, GelMA cannot be used alone, but rather must be bioprinted in composite with dECM.

3D Bioprinting with dECM-GelMA

Due to the limitations of printing with either GelMA or dECM alone, combining the two materials leverages the bioactive molecules within dECM (collagen, laminin, fibronectin, integrin) and the increased stiffness from GelMA that would not only allow for cell proliferation and differentiation, but also stable, printable constructs to create aligned fibers. While porcine ventricular-derived dECM-GelMA constructs have shown promising cell proliferation and

differentiation in human cardiac progenitor cells, this material currently remains untested in skeletal muscle-derived dECM-GelMA for C2C12 myoblasts (Bejleri et al., 2018).

Objectives

Our overarching objective was to create a hybrid biomaterial combining dECM and GelMA to mimic key structural and environmental properties as a potential bioink for printing muscle fibers to treat VML injuries. Overall, we hypothesized that dECM-GelMA would have similar physical and compositional properties to skeletal muscle and would support C2C12 viability and proliferation. We tested this hypothesis through three specific objectives:

The first objective was to engineer a decellularized dECM-GelMA material that mimicked key muscle environment properties. We hypothesized that dECM-GelMA would not contain nucleic material following the decellularization process, have a stiffness similar to muscle tissue, and contain laminin and Collagen I which are also found in muscle tissue. DNA removal was measured using DNA quantification, stiffness comparison was measured using mechanical stress testing, and protein composition was analyzed using H&E, trichrome, and immunohistochemical staining techniques.

The second objective to assess the cellular response C2C12 myoblasts to dECM-GelMA. We hypothesized that C2C12 myoblast cells seeded on top of dECM-GelMA would proliferate at a rate similar to a collagen I positive control. Proliferation was measured by counting DAPI-stained cell number per area after 24 hours of growth in a cell culture plate.

The third objective was to measure the cellular response in bioprinted constructs. We hypothesized that cells encapsulated in bioprinted dECM-GelMA constructs would maintain cell viability and proliferation. This was assessed using a proliferation assay measuring cell density over a three-day period. Through these three objectives, we will test dECM-GelMA for key

physical properties, protein content, and cell proliferation to achieve a potential printed biomaterial for VML.

Methods

Preparation of Biomaterials

dECM Preparation

Skeletal muscle quadriceps were harvested from euthanized rats. Special precautions were taken to remove excess fat and connective tissue (Figure 1A). The tissue samples were then placed in a 1% (w/v) sodium dodecyl sulfate (SDS) solution in phosphate buffer saline (PBS) and were spun at room temperature for 24 hours. SDS solution was changed once every 24 hours for three days to remove all cells from the tissue and then transferred into DI water and spun for three days, ensuring complete removal of SDS (Figure 1B). Next, tissue samples were placed in a 0.0025% solution of DNase in 10 mM MgCl2 for approximately 16-18 hours to enzymatically digest nucleic acids within the sample. At this point, the material was considered decellularized and prepared for validation testing of DNA content. To prepare the dECM to be processed into a hydrogel, the dECM was then lyophilized, milled into a fine powder (Figure 1C) and stirred in a 1 mg/mL pepsin solution in 0.1N HCl at a density of 10 mg dECM per mL pepsin solution for 48 hours. Pepsin digestion ensured the removal of large dECM pieces and production of a homogeneous mixture. The pH of the solution was then raised to 7.4 to mimic optimal cell environment through NaOH adjustment (1 N and 0.1 N) followed by the addition of 10X PBS at 10% of the solution volume for ion adjustment to a density of approximately 8 mg/mL (Figure 1D). Further density adjustments were made by adding 1X PBS and dECM solution was finally stored at 5°C.

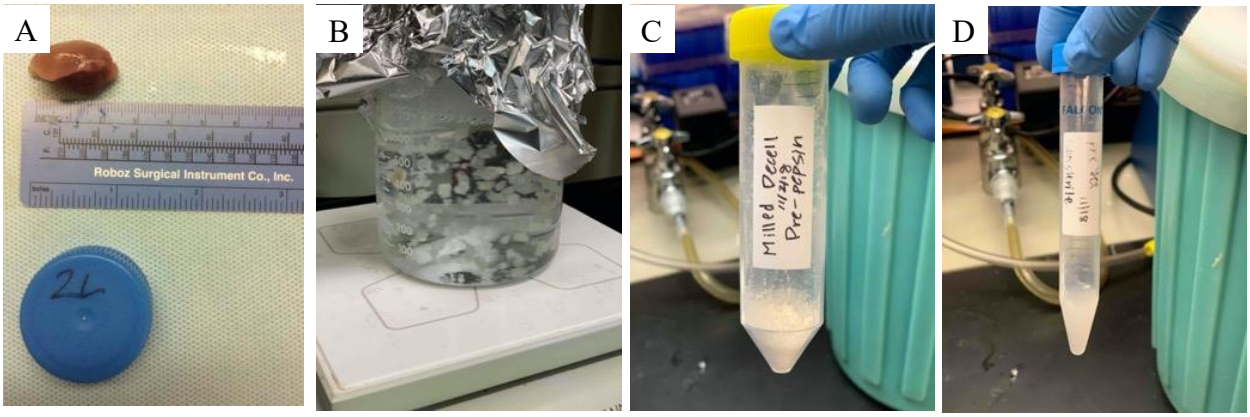

Figure 1: *Decell Pre-Gel Protocol* Following the skeletal muscle biopsy (A), muscle tissue was subject to 3 days of 1% SDS wash, 3 days of dH2O wash to remove the SDS, and 18 hours of DNase wash to remove DNA material (B). To prepare the pre-gel, dellularized tissue was frozen and milled (C) followed by pepsin digestion at 10 mg/mL. Finally, pH adjustment to 7.4 and PBS adjustment created a pre-gel with the desired concentration (D).

dECM-GelMA Preparation

Stock solutions of 15 x 10-3 M HEPES buffer solution (Sigma-Aldrich), 10 mM Eosin-Y (Santa Cruz Biotechnology), and 14.432% gelatin methacrylate (GelMA) (CellInk) in HEPES were first prepared. GelMA stock was prepared using purchased lyophilized powder reconstituted with stock concentration HEPES to reach the desired concentration. The solution was then stirred for 2 hours at 60°C and stored at -20°C for future use. The bioink consisted of 5% (w/v) GelMA, 0.75% 1-vinyl-2-pyrrolidine (NVP), 3% triethanolamine (TEOA), 100 x 10-6 M Eosin-Y and 57.3% dECM (v/v) for a total volume of 1.5 mL to form the dECM-GelMA

bioink. In cases where GelMA was tested alone, dECM was substituted for HEPES instead. All bioink components were combined immediately before printing to ensure fluidity and handling ease. To initiate the cross-linking process, the solution was placed under white light for ten minutes in 5°C. Hydrogels were stored in PBS at 37°C.

Characterization of dECM-GelMA

DNA Quantification

DNA Quantification was performed on 10-20 mg of muscle tissue, dECM, dECM-GelMA and GelMA. The QIAamp® Fast DNA Tissue Kit (Qiagen) was utilized to homogenize samples and isolate DNA, while DNA content was quantified using fluorometric quantification via the Qubit 4 Fluorometer (ThermoFisher). All samples were except muscle tissue were diluted 1:20 in Qubit® Buffer Solution. Due to the high DNA content, muscle tissue samples were serially diluted 1:10 and then 1:200 in the buffer solution for a final concentration of 1:2000.

Material Stiffness Analysis

The stiffness (Young's Modulus) was tested for muscle tissue, dECM-GelMA and GelMA using a Mach-1 V500c mechanical tester (Biomomentum). dECM-GelMA and GelMA contained 5% GelMA concentration. Cylindrical specimens approximately 10 mm in diameter and 4 mm in height were tested at room temperature (RT) up to 50% final strain at strain rate of 0.05 mm/s strain rate. Each of the cylinders was created by pipetting dECM-GelMA and GelMA into a 48-well plate in a liquid state at room temperature before gelation at 5°C under white light for ten minutes. 10mm biopsy punches were used to obtain cylindrical specimens of muscle tissue. The Young's Modulus (E) for each material was calculated from the initial linear region (0–20% of strain) of the obtained stress–strain curves using equation (1) where F is the force applied, A is the area of the material, and L is the compression length.

$$E = \frac{F}{A} * \frac{L}{\Delta L}$$

Due to the availability of materials, five dECM-GelMA hydrogels were tested while three GelMA hydrogels and two samples of muscle tissue were tested.

Histological Analysis

Muscle tissue, dECM solution, dECM-GelMA hydrogel, and GelMA hydrogel were frozen at -20C and sliced in 10-20 μM sections using a cryostat microtome and placed on glass slides. Cryosections were fixed with 4% paraformaldehyde and stained with hematoxylin and eosin (H&E) (Poly Scientific, Bayshore, NY) or Gomori's Trichrome (Polysciences, Warrington, PA) to further assess collagen content. Sections were analyzed using light microscopy (Zeiss, Oberkochen, Germany).

Immunohistochemical Analysis

Cryosections were fixed with 4% paraformaldehyde in PBS for 15 min. Following a PBS wash, sections were blocked with 2% bovine serum albumin (BSA), 0.5% goat serum, 0.5% Triton X-100 in PBS at 4 degrees overnight. After a PBST (0.1% Tween) wash, sections were incubated with Anti-Laminin rabbit primary antibody (Abcam) and Anti-Collagen I mouse primary antibody (ab6308, Abcam). Following a wash in PBST, laminin and collagen stained sections were labeled with Alexa-Fluor® 555 goat anti-Rabbit secondary antibody IgG (H+L) (ThermoFisher) and Alexa-Fluor® 647 goat anti-mouse secondary antibody IgG (H+L) (ThermoFisher). Slides were mounted with Vectashield Mounting Medium with DAPI and imaged with a fluorescent microscope (Zeiss, Oberkochen, Germany)

Proliferation of C2C12 in Non-Printed dECM-GelMA Hydrogel

Cell proliferation on dECM coating was compared against rat tail collagen I (Sigma-Aldrich), agarose as a negative control, and a non-coated plastic well plate as a positive control.

To coat tissue culture plastic, 250 uL of each material was placed into a 24-well plate in triplicate and incubated at 37°C for 30 minutes. Next dECM solution and the collagen I solution aspirated, and any excess was allowed to evaporate, creating a thin protein coating on the plate. dECM was plated at a concentration of 10 mg/mL and collagen I was plated at a concentration of 0.3 ug/mL.

To test C2C12 hydrogel proliferation, 250 uL of dECM-GelMA, GelMA, Bovine collagen I gel (Advanced Biomatrix) at 5 mg/mL, and agarose gel were plated onto a 24-well plate in triplicate and allowed to gelate overnight at 5°C. Next, C2C12s were seeded at a density of 20,000 cells/well and allowed to grow for 24 hours. Finally, cells were fixed in 4% PFA for 10 minutes, washed in PBS, and stained with Hoechst and imaged with a fluorescence microscope (Samples were analyzed using light microscopy (Zeiss, Oberkochen, Germany). Proliferation was quantified by # cells/mm^2 using ImageJ.

Proliferation of C2C12 in Printed dECM-GelMA Constructs

3D-Printing

The following procedure utilized a commercial bioprinter (EnvisionTEC 3D-bioplotter Developer Series) and was adapted from Bejleri et al. 1.5 mL of bioink was added to a 30cc printer barrel fitted with a 27-gauge plastic needle tip. The barrel was added to the printer head and cooled to 10°C. The printing shape followed a template designed by Davis Lab designed to optimize cell nutrient infiltration.(Bejleri et al., 2018) Each disk was 1 cm in diameter and 1 mm in height with a .5 mm-thick grid in-fill layout. Patches were printed on a glass slide with a pressure of 0.8-1.0 bar at 10 mm/s. Following printing, the patches were placed under white light for five minutes to induce polymerization and stored at 37°C.

C2C12 Proliferation

To assess proliferation of C2C12 encapsulated in dECM-GelMA printed patches, samples were stained for Hoechst and imaged via the Fluoview FV3000 confocal laser scanning microscope (Olympus, Tokyo, Japan) and cells were counted and analyzed in ImageJ. To get a representative count of cells throughout each sample, a z-stack image was taken at two locations in each sample, and two sections were randomly selected from each z-stack image for a total of four images per construct. 20 sections each approximately 50 μm in height were taken to cover the entire millimeter height of the print and prevent cell overlap between images. Constructs were tested in triplicate immediately after print (Day 0), after 24 hours (Day 1), and after three days (Day 3). Cell proliferation was determined by the average number of Hoechst stained cells per mm^2. Because of the porous nature of the constructs, cells were only distributed throughout the grid layout of the patch rather the entire objective. To account for the variable area the patch covered in each image, samples were normalized to the occupied dECM-GelMA surface area rather than the entire area of the image.

Statistics

Numerical data are presented by the mean ± SD. All data except for mechanical analysis was analyzed using one-way ANOVAs with Tukey's post-test with sample size n=3. Due to the low sample size of muscle tissue in mechanical testing, it did not fit the criterion of ANOVA. Instead unpaired t-tests were used to compare between muscle tissue (n=2), GelMA (n=3) and dECM-GelMA (n=3).

Results

DNA Quantification

DNA content in muscle tissue was determined to be 764.37±42.89 ng/mg (Figure 1A). Because the DNA content for dECM, dECM-GelMA, and GelMA fell out of the sensitivity range of the fluorometer (<0.5 ng/mL), their DNA content was approximated from the initial mass of each sample, factoring in the dilution from the extraction process and subsequent quantification process. All results were found to be statistically significantly against muscle tissue. DNA removal was further confirmed with immunofluorescence staining with DAPI (Figure IB). Only muscle tissue stained samples qualitatively showed marked nuclei, suggesting the removal of cellular material from dECM, dECM-GelMA, and GelMA.

A

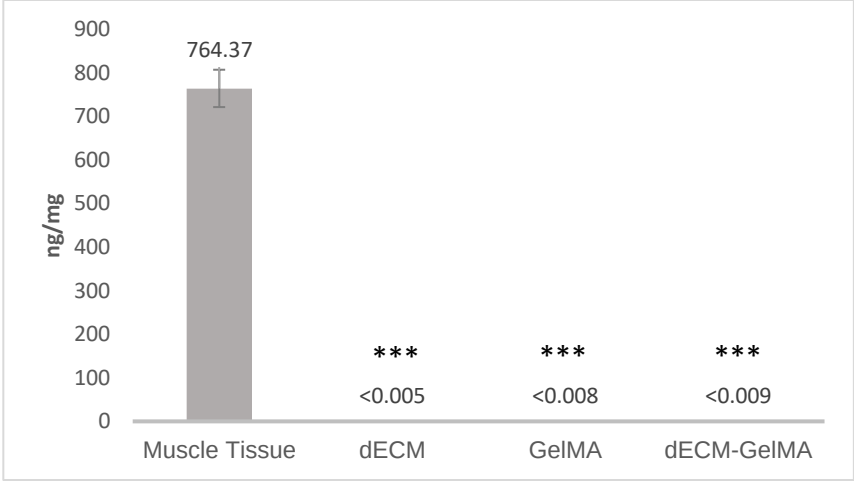

B

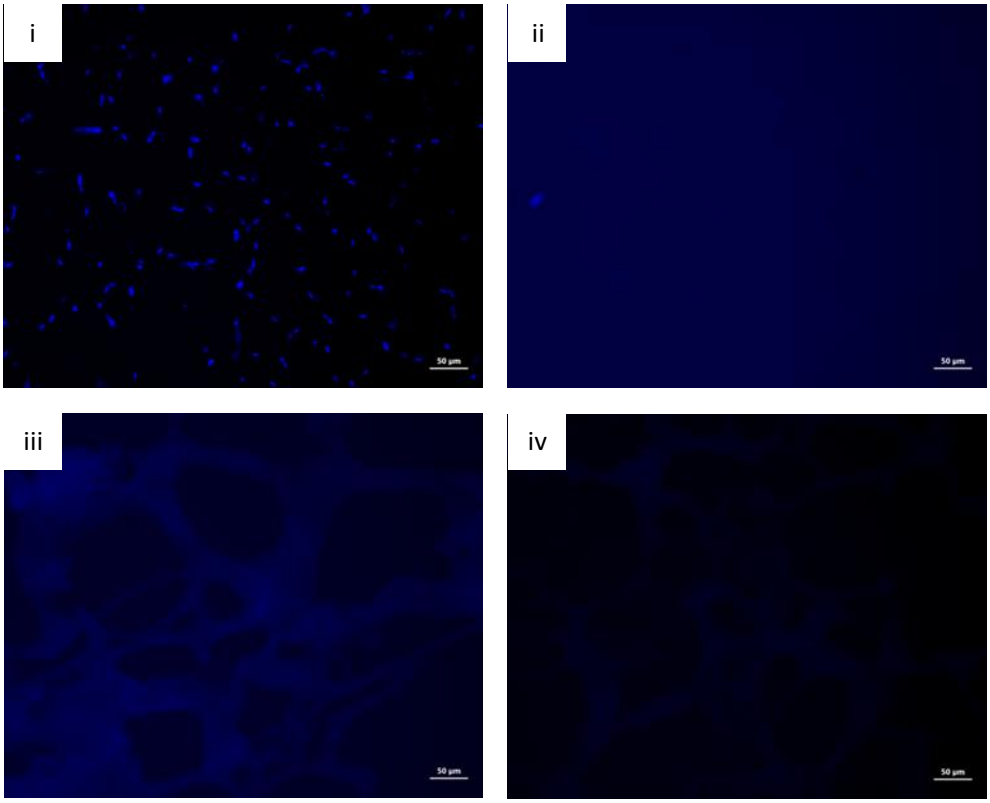

Figure 2: Quantification of DNA Removal A) DNA content extracted with QIAamp Fast DNA Tissue Kit and analyzed with Qubit 4 Fluorometer (n=3) (***p<.0001 using ANOVA with Tukey post-test, n=3) B) DAPI stained histology sections of i) Muscle Tissue ii) dECM iii) dECM-GelMA, and iv) GelMA.

Mechanical Testing

Material stiffness plays an important role in C2C12 differentiation when encapsulated in a hydrogel matrix. dECM-GelMA not significantly different to muscle tissue at 5.4 kPA and 4.9 kPa, respectively, at low strain rates. Furthermore dECM-GelMA had a significantly stiffer modulus than GelMA at 2.6 kPa, indicating that the addition of dECM added further stiffness to GelMA alone (Figure 3A). Due to material availability there were lower sample sizes of muscle tissue (n=2) and GelMA (n=3) and in future work more samples will be run to fully power this experiment. In addition, GelMA was noticeably fragile, resulting in a lower sample size. dECM, due to its liquid state, was unable to be mechanically tested.

A

B

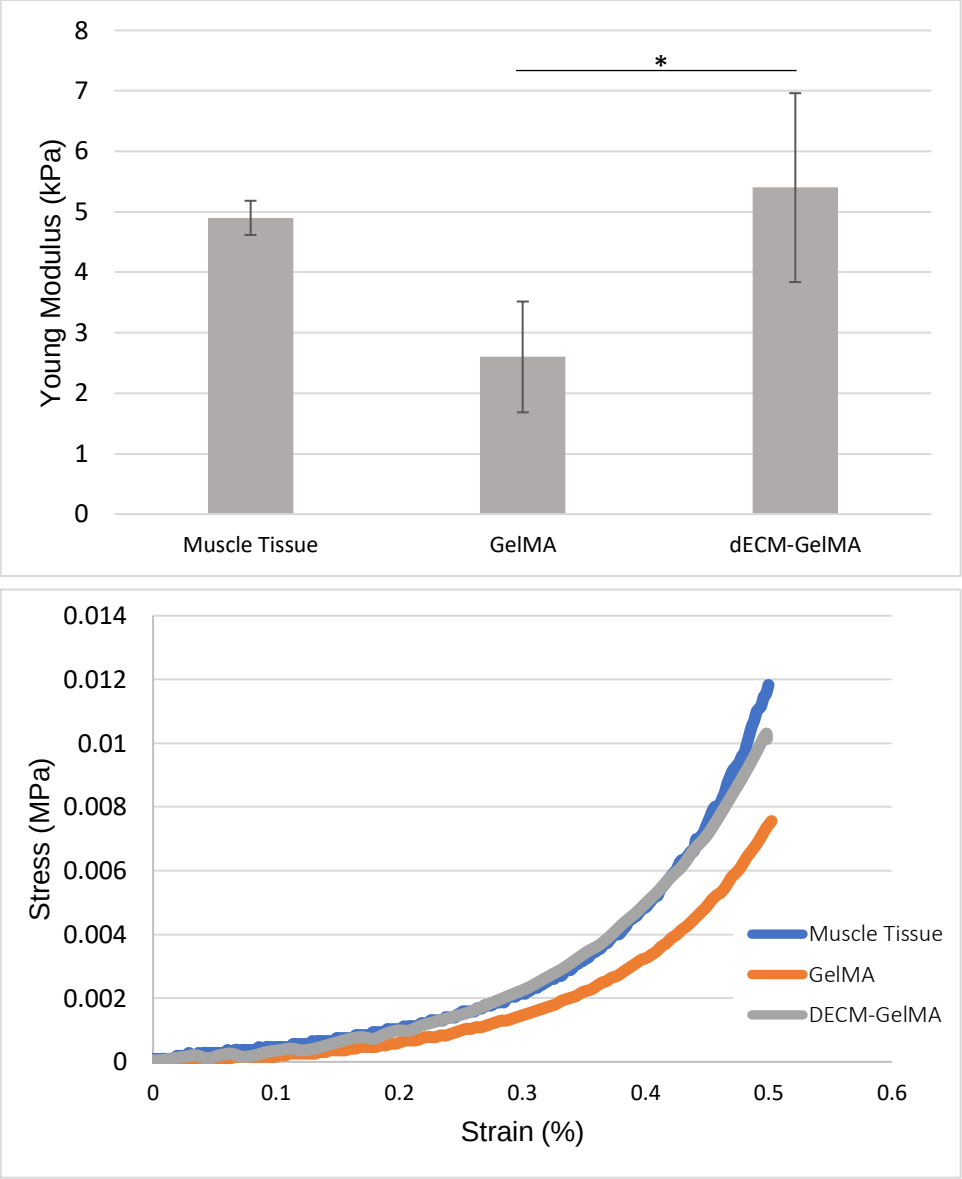

Figure 3: A) *Stress vs Strain Curve* Samples were measured along the 20% linear strain range of the Stress vs Strain curve and the modulus was determined by taking the slope of the best-fit line. B) *Quantification of Young's Modulus* dECM-GelMA (n=5), GelMA (n=3), and Muscle Tissue (n=2) samples approximately 10 mm in diameter and 4 mm in height were analyzed in the initial 20% strain range. GelMA concentrations were 5% (w/v). dECM-GelMA samples were found to not be significant from muscle tissue but significant compared to GelMA. (*p<.05 using unpaired t-test)

dECM-GelMA Content Characterization

H&E and Trichrome Staining

Hematoxylin and Eosin (H&E) staining of sectioned samples revealed the presence of nucleic material stained blue in muscle tissue and confirmed the lack of DNA content in dECM, dECM-GelMA, and GelMA (Figure 4A). Eosin, which stains for cytoplasmic proteins, qualitatively showed the presence of protein in dECM. Trichrome staining further specified the protein characterization of the samples. Nuclei was stained black, cytoplasm, keratin, muscle fibers were stained red, and collagen was stained a greenish blue. In the muscle tissue sample, the perimysium or the elastic tissue surrounding a muscle group is clearly distinguished by the light blue segment running across the image, indicated by the blue arrow (Figure 4BI). Collagen content was also confirmed in the dECM sample, which was stained only blue (Figure 4BII). Finally, specific protein content was difficult to extrapolate in the two GelMA samples due to the non-specific staining in the red channel.

Immunohistochemical Staining

In order to further elucidate protein content, samples were stained for collagen I and laminin. Collagen I was clearly detected once again along the perimysium in muscle tissue and surrounding individual muscle fibers, indicated by the blue arrow (Figure 5I). dECM did not fluoresce at all, indicating the absence of collagen I (Figure 5II). dECM-GelMA and GelMA samples displayed fluorescence for collagen I, though the lack of punctate signal and unstained control sample, it was difficult to extrapolate whether the samples actually contained collagen I or were instead displaying background fluorescence.

Laminin content was clearly detected in muscle tissue and dECM, indicated by the blue arrows (Figure 6II) but were not clearly found in GelMA or dECM-GelMA. dECM-GelMA, did

noticeably present a higher signal when tested under identical imaging conditions to GelMA though it is unconfirmed whether this is due to trace amounts of laminin. It is important to note that due to the high water content of each dECM and GelMA, there were significant challenges in producing testable samples via cryosectioning, resulting in a lower than optimal sampling range and freeze artifacts within the samples.

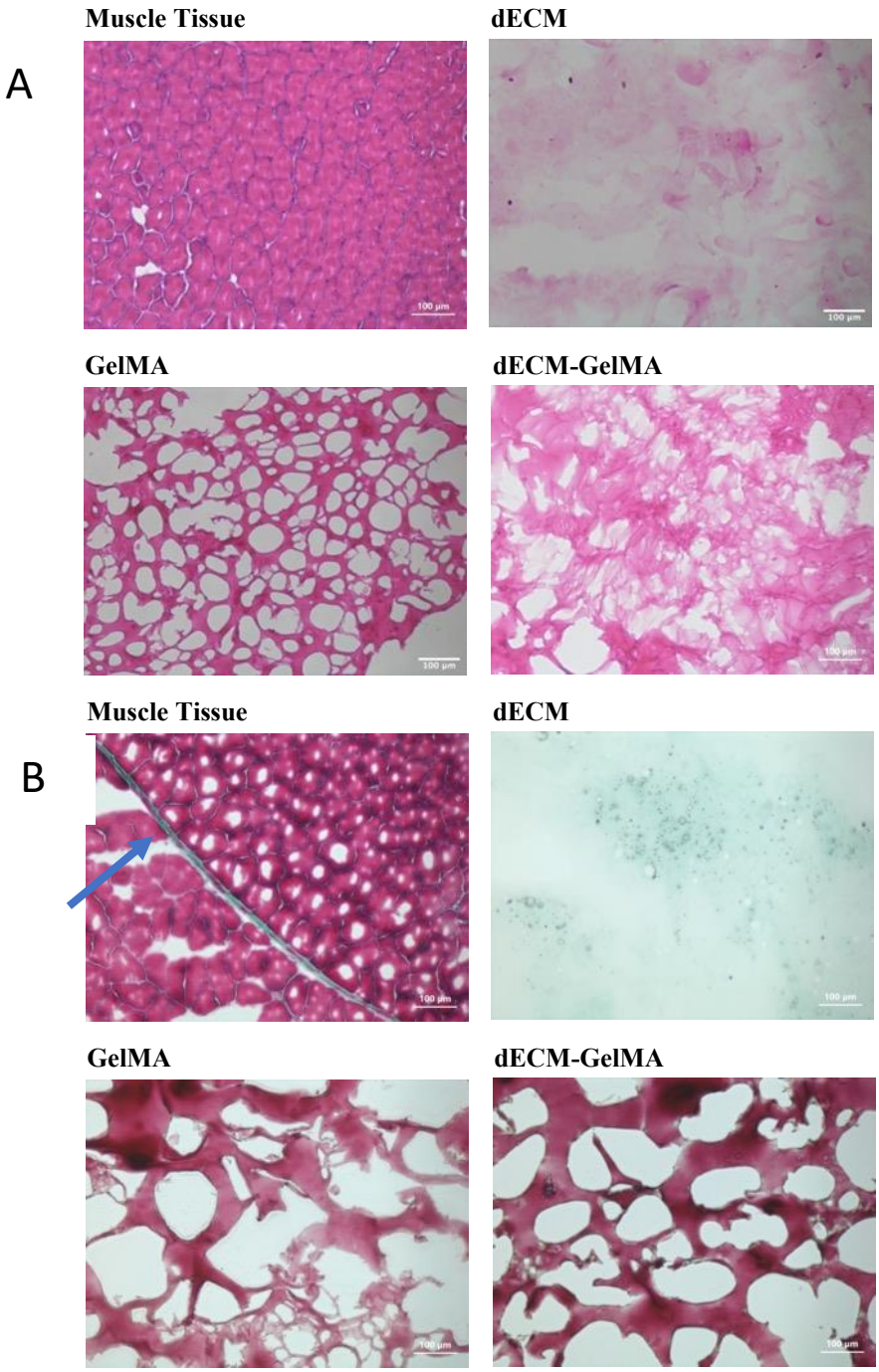

Figure 4: A) *H&E Staining* Histological sections of muscle tissue highlights individual muscle fibers and nuclei (hematoxylin blue) as well as lack of nucleic material in all other samples. Unspecified proteins were also stained pink with eosin. B) *Gomori's Trichrome Staining* Light blue staining indicates presence of unspecified collagen, clearly displayed in muscle tissue (blue arrow) and dECM.

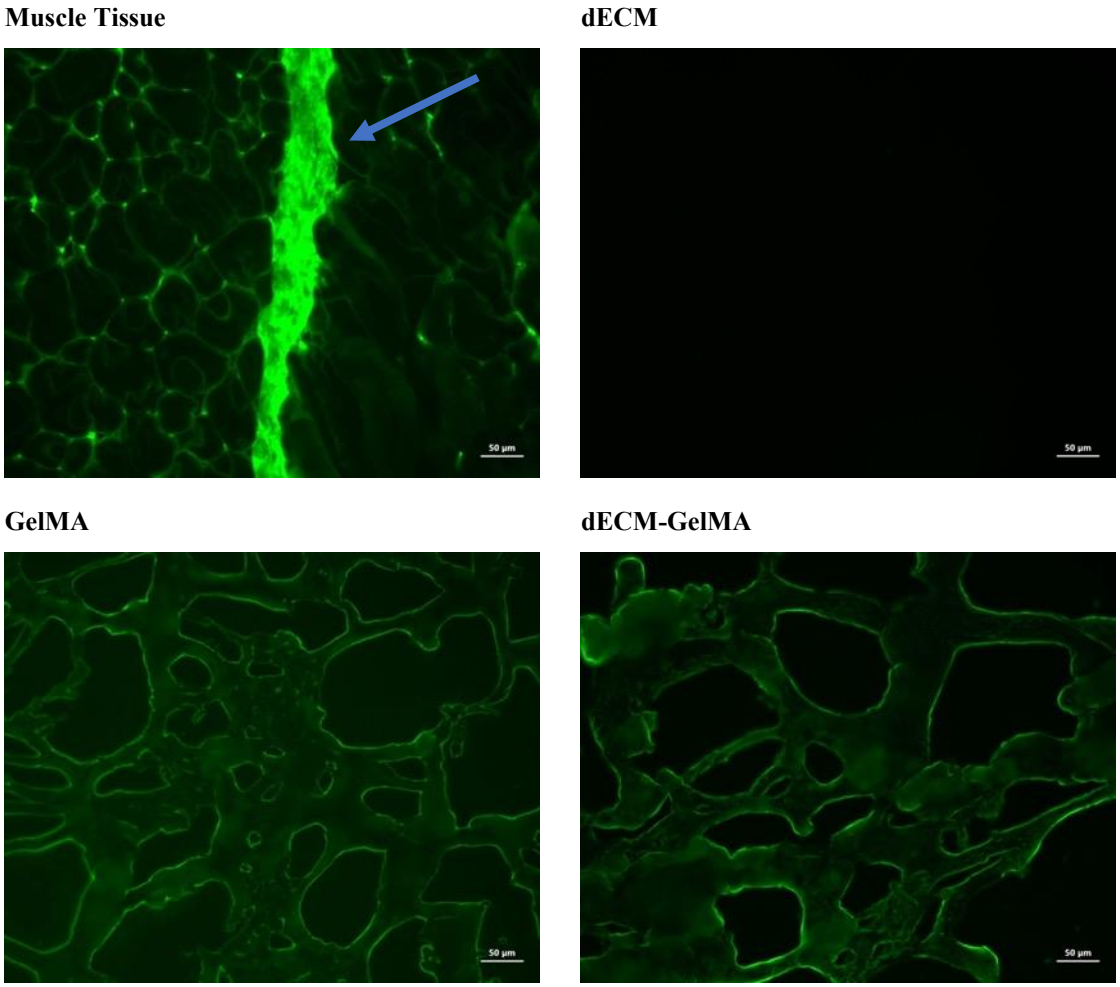

Figure 5: *IHC Staining for Collagen I* Fluorescence for collagen I is clearly displayed along the perimysium in muscle tissue and borders of individual muscle fibers, indicated by the blue arrow. Fluorescence is also clearly displayed in both GelMA samples along the border of the material, suggesting the presence of collagen as well. However, collagen I was not expressed in dECM.

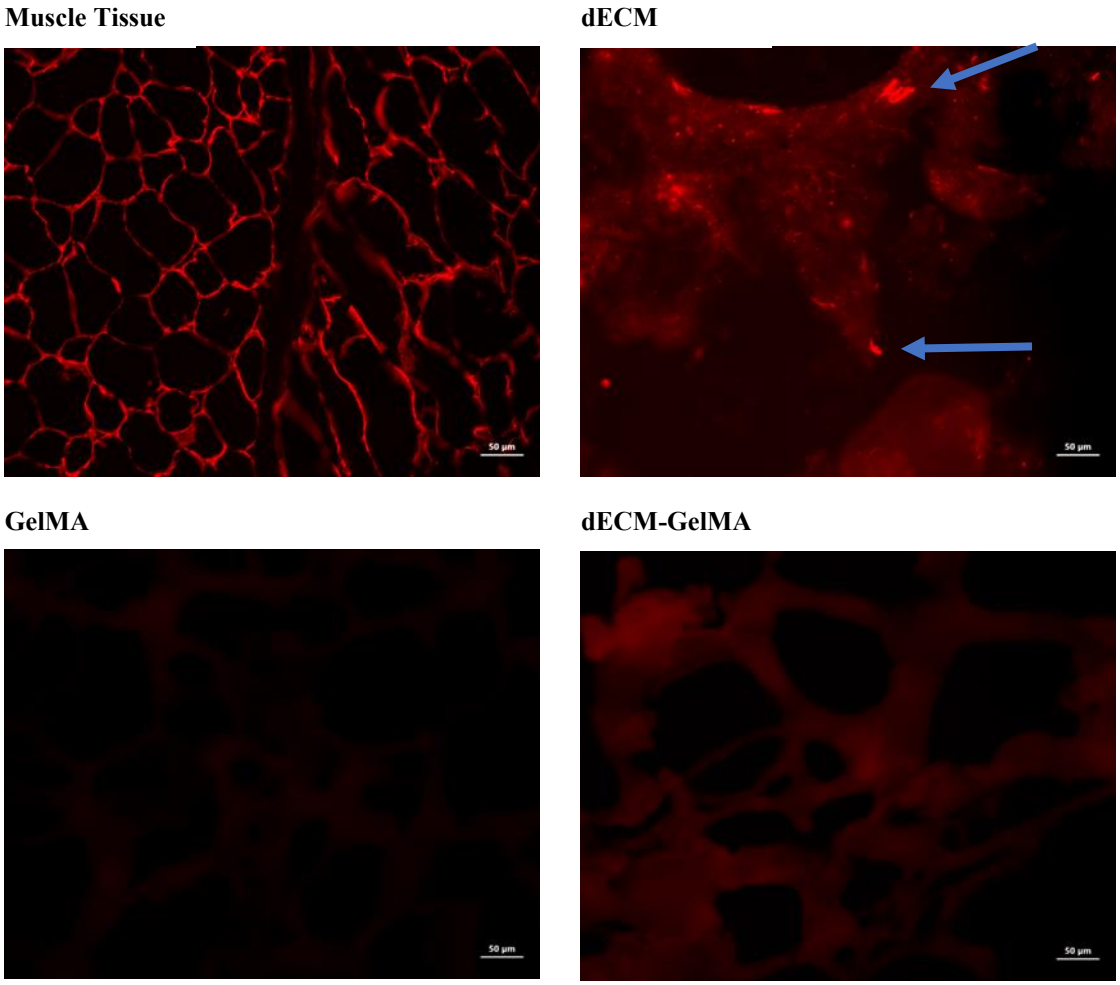

Figure 6: *IHC Staining for Laminin* Fluorescence for laminin is clearly surrounding muscle fibers in muscle tissue and distributed throughout dECM, indicated by the blue arrows. While dECM-GelMA samples did fluoresce brighter than GelMA, it could not be exactly identified as containing laminin.

Proliferation in C2C12 in dECM and dECM-GelMA

To assess cell proliferation in the dECM coated plate alone, the cell density, calculated by cell number per mm^2, was measured after 24 hours under four different conditions: A non-coated plastic bottom positive control, an agarose gel negative control, collagen I, and dECM (Figure 4A). Cell density in dECM was found to be statistically higher than in the agarose negative control, but not significant against the positive control, indicating that cell proliferated in dECM as well as in a tissue culture plate. In addition, cell number in dECM also increased against the initial seeding density of approximately 105 cells per mm^2, which was calculated by dividing the well area by the image area, resulting in an average of 205±6.03 cell/mm^2.

To assess cell density in dECM-GelMA hydrogel, cell density was instead compared against a collagen I gel positive control, agarose gel negative control, and dECM-GelMA hydrogel (Figure 4B). dECM-GelMA hydrogel was also found to be significant higher when compared against the negative control, but not significant against the collagen I gel positive control. However, cell density in the dECM-GelMA hydrogel decreased slightly from the initial seeding density at 74.9±14.0 cell/mm^2.

A

Tissue Culture Plate

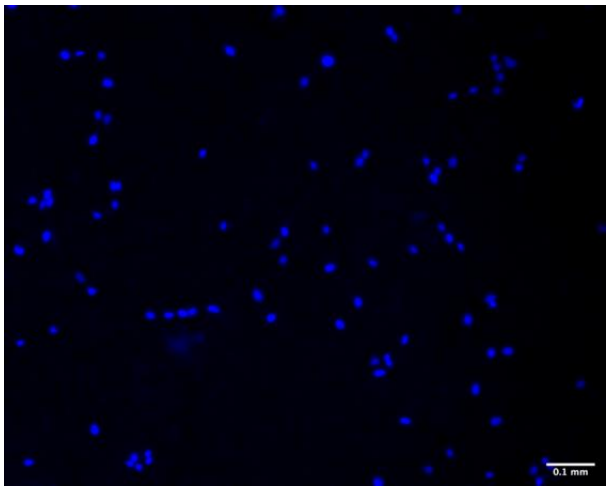

Agarose

Collagen I Coat

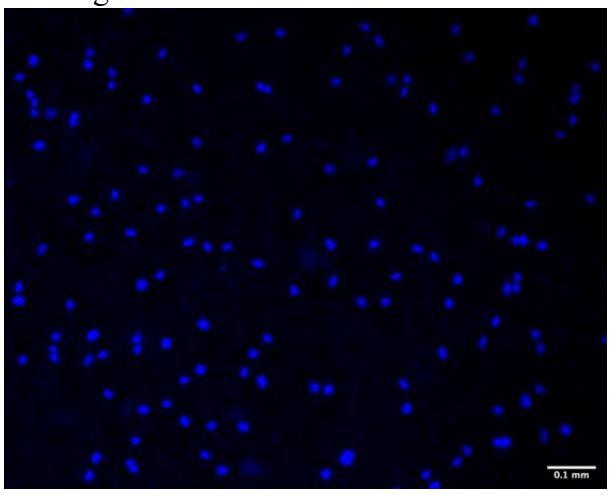

dECM Coat

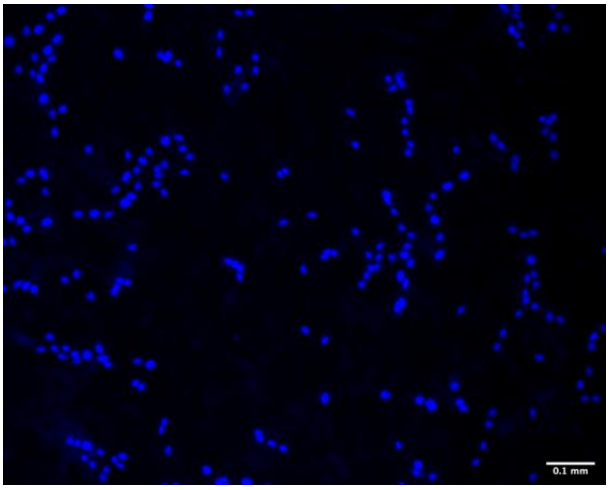

B

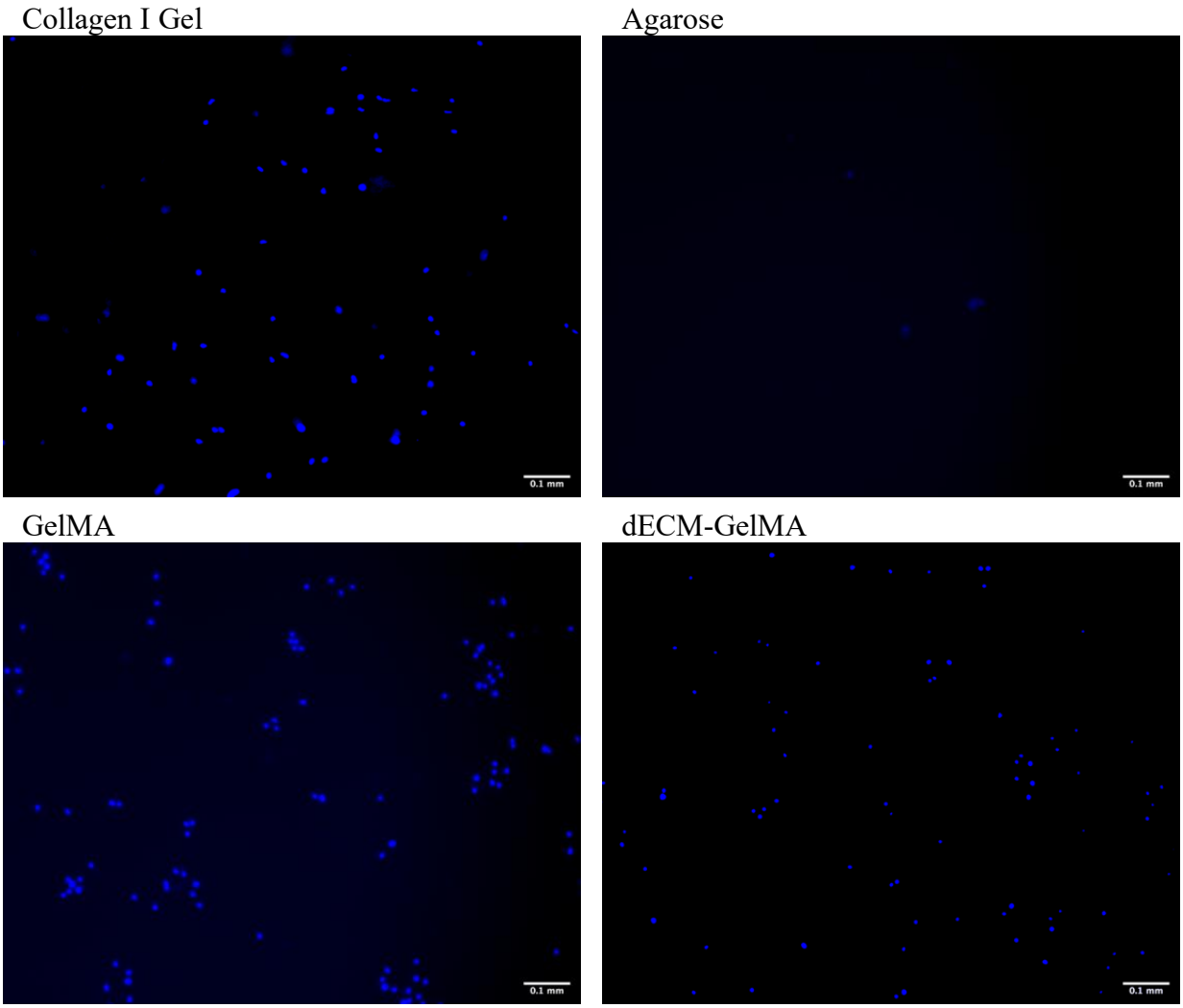

Figure 7: A) *Hoechst Images of Protein Coated Wells* B) *Hoechst Images of Gel Coated Wells* All images taken 24 hours after seeding on top of materials.
(Scale Bar = 0.1mm for all images)

A

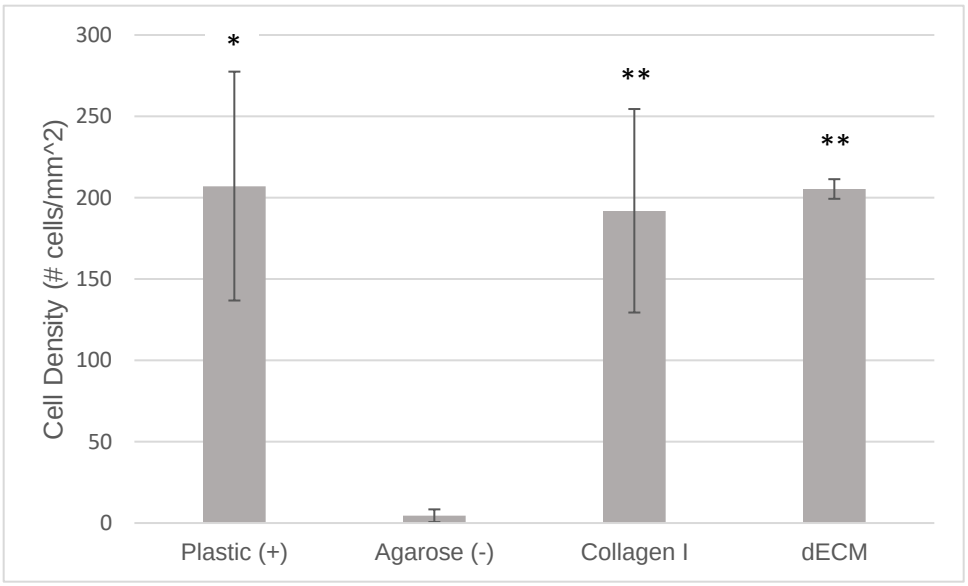

B

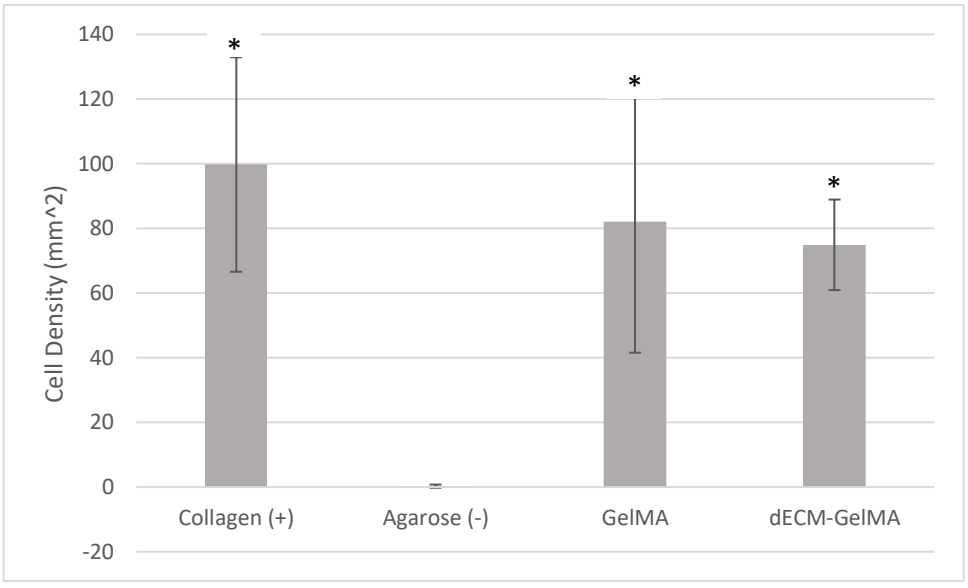

Figure 8: A) *Cell Proliferation of dECM Coated Plate* C2C12 proliferation on dECM was tested against a non-coated plastic surface, collagen I and agarose gel. B) *Cell Proliferation of dECM-GelMA gel.* All samples were seeded at an initial seeding density of 20,000 cells/well (105 cells/mm2). Cell density was measured after 24 hours for both assays. (*p<.05, **p<.005 against negative control using ANOVA with Tukey's post-test, n=3)

Proliferation in dECM-GelMA Printed Constructs

Cell density significantly increased during this time starting from 295±52 cells/mm2 to 415±81 cells/mm2, indicating that cells were able to proliferate in the dECM-GelMA environment. In addition, printed constructs remained structurally stable through the three days, maintaining handling ease and integrity.

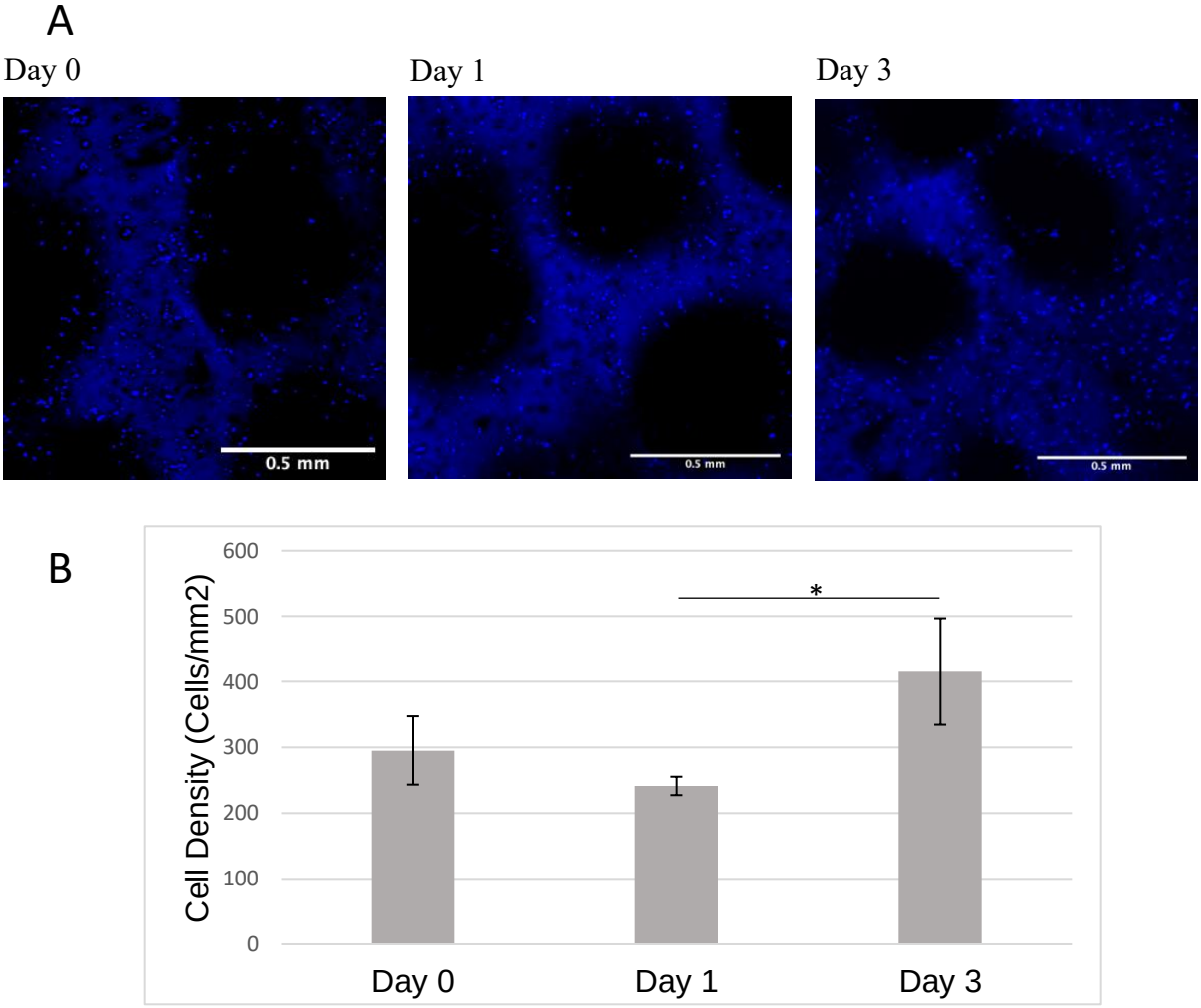

Figure 9: A) *Hoechst Images of Cell Density at Day 0, 1, and 3*. B) *Cell proliferation in dECM-GelMA Patch* Cell count was determined from Hoechst stained nuclei and normalized against the area of the patch. Cell density did not significantly increase after the first day but did significantly increase from Day 1 at Day 3. (*p<.05 using ANOVA with Tukey's post-test, n=3 for all groups)

Discussion

In order to utilize a prospective material as a tissue engineering treatment for volumetric loss, the material must mimic the native environment of the skeletal muscle ECM. Successful replication of this matrix requires the presence of similar environmental cues that allow the successful long-term proliferation and differentiation of transplanted muscle stem cells. These cues not only include the presence of ECM proteins including collagen and laminin, but also physical conditions that would allow for optimal differentiated and aligned muscle fibers.

In this thesis, we developed and tested a new biomaterial, dECM-GelMA, for potential muscle tissue engineering applications. This material is ideal for skeletal muscle tissue engineering as its stiffness can be manipulated through the use of gelatin methacrylate, it can be 3D bioprinted which provides an additional layer of organization that has been found to successfully align muscle fibers, and dECM incorporates the native cell adhesion proteins found in skeletal muscle. The objective for this thesis was to develop a fabrication method for dECM-GelMA hydrogels and characterize the material following the criterion for muscle tissue ECM. In addressing our first objective, DNA quantification confirmed the successful removal of DNA content and mechanical testing determined that dECM-GelMA was statistically similar to muscle tissue, proving that the material contained the optimal environment for cell differentiation. These both supported our hypothesis that ECM-GelMA would not contain nucleic material following the decellularization process and would have a stiffness similar to muscle tissue, matching the criterion outlined by Engler et al.. Because dECM on its own did not gelate, it was not included in mechanical testing, although it did contribute in increasing the stiffness of dECM-GelMA. ECM Protein content characterization confirmed the presence of collagen I and laminin in muscle tissue as well as laminin in dECM alone. However, due to time constraints and available

materials, there were significant limitations to the extent the protein content of the samples could be analyzed. While the images were able to provide some context to the protein content, they could not be fully quantified. Further analysis would include a Western Blot assay to quantify dECM-GelMA for collagen I, laminin, and other extracellular proteins such as laminin and fibronectin. In addition, collagen IV, known to be abundant in muscle tissue would also be imaged and quantified. While collagen I immunofluorescence was detected in both GelMA sample types, without the presence of an unstained control, it was difficult to draw conclusions as to whether the samples truly contained collagen I.

To test our second objective was on cell survival on the surface of dECM-GelMA, cell density was measured over a 24 hour period on dECM and dECM-GelMA. While cell count in dECM alone nearly doubled from the starting seeding density, the cell count remained not significant from the starting density in both GelMA types. However, the positive control collagen I construct also remained similar to the starting density and statistically similar to the GelMA types, indicating that proliferation was most likely decreased in a gel environment. This supported the hypothesis that seeded cells would not display a significantly different cell density to our positive control. Finally, our third objective was to test proliferation in dECM-GelMA. In printed constructs cell density nearly doubled within the three-day testing period, addressing our third hypothesis that cells encapsulate in dECM-GelMA would sustain proliferation. Overall, printed constructs maintained their integrity over the three-day period, proving the efficacy of GelMA as a viable support structure for dECM. This supports the findings presented by Bejleri et al. and could potentially address the issues of cell alignment introduced by Aurora et al.. While multiple further studies for each would be required to fully optimize the printing process

for cell viability and proliferation, the results provide a solid framework for a printable dECM-GelMA bioink protocol.

Conclusion and Future Directions

Overall, a protocol was developed for a successfully decellularized dECM-GelMA material that presented an ideal stiffness, comparable to muscle tissue. In addition, the material was also adapted for 3D-printing purposes, successfully created stable constructs that could be measured and quantified over three-days in cell culture conditions without degradation or significant handling difficulty in comparison to dECM alone. While the study presented a broad overview of cellular response and protein content within dECM-GelMA, future experiments would provide a more in-depth and varied look at the exact protein characterizations of dECM and dECM-GelMA. Further analysis would include a Western Blot assay to quantify dECM-GelMA for collagen I, laminin, and other extracellular proteins such as fibronectin and collagen IV, known to be abundant in muscle tissue. In addition, secondary staining controls would be included for ICC staining to better separate protein detection from background autofluorescence.

Because laminin was clearly detected in dECM, in future studies, we would include a laminin coated experimental group to compare cell proliferation against proliferation on a dECM surface. Furthermore, incorporating laminin into GelMA hydrogels and comparing proliferation against dECM-GelMA would help elucidate the role laminin plays in promoting cell adhesion and proliferation in bioprinted hydrogels. It is important to note that cell density did decrease after day one before rising again after day three, suggesting that cells may have required time to acclimate to a new environment. Future studies would investigate this cell interaction further, including testing the 48-hour timepoint to pinpoint when proliferation increases.

Finally, because the cellular response experiments focused on cell proliferation, future experiments would instead examine C2C12 differentiation in dECM and dECM-GelMA. As we hypothesized that printed constructs would be key in providing cell alignment, examining cell differentiation would be necessary to prove the muscle fiber alignment via the physical patterning of the patches. In order to test this, a similar setup to the 24-well proliferation assay would be conducted, but instead extended over a week-long timeframe, to allow cells to reach adequate confluency for differentiation. Next, a similar experiment would be conducted in printed constructs as well. By staining samples for actin and myosin, not only would the cell morphology of the C2C12 in these environments be further elucidated, but the presence of aligned myotubes would be able to be identified and quantified. Volumetric muscle loss continues to be a significant injury, severely impacting the mobility and quality of life for those affected. Without existing treatments to regenerate functional muscle, creating artificial dECM scaffolds currently remains a promising tissue engineering strategy. The results shown here offer a potential therapeutic treatment for VML by creating a new dECM-GelMA hybrid biomaterial for use in 3D bioprinting applications.

Reference Cited

Aurora, A., Roe, J. L., Corona, B. T., & Walters, T. J. (2015). Biomaterials An acellular biologic scaffold does not regenerate appreciable de novo muscle tissue in rat models of volumetric muscle loss injury. *Biomaterials*, *67*, 393–407. https://doi.org/10.1016/j.biomaterials.2015.07.040

Bahney, C. S., Lujan, T. J., Hsu, C. W., Bottlang, M., West, J. K., & Johnstone, B. (n.d.). Visible Light Photoinitiation of Mesenchymal Stem Cell-Laden Bioresponsive Hydrogels.

Bejleri, D., Streeter, B. W., Nachlas, A. L. Y., Brown, M. E., Gaetani, R., Christman, K. L., &

Davis, M. E. (2018). A Bioprinted Cardiac Patch Composed of Cardiac-Specific Extracellular Matrix and Progenitor Cells for Heart Repair. *Advanced Healthcare Materials*, *1800672*, 1800672. https://doi.org/10.1002/adhm.201800672

Bentzinger, C. F., Wang, Y. X., Dumont, N. A., & Rudnicki, M. A. (2013). Cellular dynamics in the muscle satellite cell niche. *Nature Publishing Group*, *14*(12), 1062–1072. https://doi.org/10.1038/embor.2013.182

Brown, B. N., Valentin, J. E., Stewart-akers, A. M., Mccabe, G. P., & Badylak, S. F. (2009). Biomaterials Macrophage phenotype and remodeling outcomes in response to biologic scaffolds with and without a cellular component. *Biomaterials*, *30*(8), 1482–1491. https://doi.org/10.1016/j.biomaterials.2008.11.040

Choi, Y. J., Kim, T. G., Jeong, J., Yi, H. G., Park, J. W., Hwang, W., & Cho, D. W. (2016). 3D Cell Printing of Functional Skeletal Muscle Constructs Using Skeletal Muscle-Derived Bioink. *Advanced Healthcare Materials*, *5*(20), 2636–2645. https://doi.org/10.1002/adhm.201600483

Choi, Y., Jun, Y., Yeon, D., Yi, H., Chae, S., Rhie, J., & Cho, D. (2019). Biomaterials A 3D cell printed muscle construct with tissue-derived bioink for the treatment of volumetric muscle loss. *Biomaterials*, *206*(March), 160–169. https://doi.org/10.1016/j.biomaterials.2019.03.036

Engler, A. J., Griffin, M. A., Sen, S., Bönnemann, C. G., Sweeney, H. L., & Discher, D. E. (2004). Myotubes differentiate optimally on substrates with tissue-like stiffness : pathological implications for soft or stiff microenvironments, *166*(6), 877–887. https://doi.org/10.1083/jcb.200405004

Grasman, J. M., Zayas, M. J., Page, R., & Pins, G. D. (2015). Biomimetic Scaffolds for

Regeneration of Volumetric Muscle Loss in Skeletal Muscle Injuries. *Acta Biomater*, *25*, 2–15. https://doi.org/10.1016/j.actbio.2015.07.038.Biomimetic

Kim, J. H., Seol, Y. J., Ko, I. K., Kang, H. W., Lee, Y. K., Yoo, J. J., … Lee, S. J. (2018). 3D Bioprinted Human Skeletal Muscle Constructs for Muscle Function Restoration. *Scientific Reports*, *8*(1), 1–15. https://doi.org/10.1038/s41598-018-29968-5

Lee, H., Min, Y., Kim, I., Elsangeedy, E., Ho, J., Yoo, J. J., … Jin, S. (2020). A novel decellularized skeletal muscle-derived ECM scaffolding system for in situ muscle regeneration. *Methods*, *171*(July 2019), 77–85. https://doi.org/10.1016/j.ymeth.2019.06.027

Melo, F., Carey, D. J., & Brandan, E. (1996). Extracellular Matrix I s Required for Skeletal Muscle Differentiation But Not Myogenin Expression, *239*(1 996), 227–239.

Noshadi, I., Hong, S., Sullivan, K. E., Sani, E. S., Portillo-lara, R., Tamayol, A., … Annabi, N. (2017). In vitro and in vivo analysis of visible light crosslinkable gelatin methacryloyl (GelMA) hydrogels. https://doi.org/10.1039/c7bm00110j

Ostrovidov, S., Hosseini, V., Ahadian, S., Fujie, T., Parthiban, S. P., Ramalingam, M., … Khademhosseini, A. (2014). Skeletal Muscle Tissue Engineering : Methods to Form Skeletal Myotubes, *20*(5), 403–436. https://doi.org/10.1089/ten.teb.2013.0534

Pati, F., Jang, J., Ha, D. H., Won Kim, S., Rhie, J. W., Shim, J. H., … Cho, D. W. (2014). Printing three-dimensional tissue analogues with decellularized extracellular matrix bioink. *Nature Communications*, *5*, 1–11. https://doi.org/10.1038/ncomms4935

Sackett, S. D., Tremmel, D. M., Ma, F., Feeney, A. K., Mag, R. M., Brown, M. E., … Odorico, J. S. (2018). Extracellular matrix scaffold and hydrogel derived from decellularized and delipidized human pancreas, (April), 1–16. https://doi.org/10.1038/s41598-018-28857-1

Spang, M. T., & Christman, K. L. (2018). Extracellular matrix hydrogel therapies: In vivo

applications and development. *Acta Biomaterialia*, *68*, 1–14. https://doi.org/10.1016/j.actbio.2017.12.019

Theocharis, A. D., Skandalis, S. S., Gialeli, C., & Karamanos, N. K. (2016). Extracellular matrix structure ☆. *Advanced Drug Delivery Reviews*, *97*, 4–27. https://doi.org/10.1016/j.addr.2015.11.001

Vorotnikova, E., Mcintosh, D., Dewilde, A., Zhang, J., Reing, J. E., Zhang, L., … Braunhut, S. J. (2010). Extracellular matrix-derived products modulate endothelial and progenitor cell migration and proliferation in vitro and stimulate regenerative healing in vivo. *Matrix Biology*, *29*(8), 690–700. https://doi.org/10.1016/j.matbio.2010.08.007

Wang, Y. X., Dumont, N. A., & Rudnicki, M. A. (2014). CELL SCIENCE AT A GLANCE Muscle stem cells at a glance, 4543–4548. https://doi.org/10.1242/jcs.151209

Yue, K., Santiago, G. T., Tamayol, A., Annabi, N., Khademhosseini, A., Hospital, W., & Arabia, S. (2016). Synthesis, Properties, and Biomedical Applications of Gelatin Methacryloyl (GelMA) Hydrogels, 254–271. https://doi.org/10.1016/j.biomaterials.2015.08.045.Synthesis